Electronic Supplementary Material (ESI) for Analyst.


## Supporting Information

# High-Fidelity Imaging of Intracellular MicroRNA via a Bioorthogonal Nanoprobe

*Hengyi Chen [a#], Xiaohui Chen [a, b#], Yi Chen [a#], Chong Zhang [b], Zixin Sun [a], Jiaxi Mo [e], Yongzhong Wang [b], Jichun Yang [a]*, Dongsheng zou [f]*, Yang Luo [a, c, d]**

[a]Center of Smart Laboratory and Molecular Medicine, School of Medicine, Chongqing University, Chongqing, 400044, P.R. China.
[b]Key Laboratory for Biorheological Science and Technology of Ministry of Education, College of Bioengineering, Chongqing University, Chongqing, 400044, P.R. China.
[c]College of Life Science and Laboratory Medicine, Kunming Medical University, Kunming, Yunnan, 650050, P.R. China.
[d]Department of Laboratory Medicine, Third Affiliated Hospital of Kunming Medical University (Tumor Hospital of Yunnan Province), Kunming, Yunnan, 650118, P.R. China.
[e]School of Clinical Medicine, Southwest Medical University, Luzhou, Sichuan, 646000, P.R. China.
[f]College of Computer Science, Chongqing University Chongqing, 400044, China

#These authors contributed equally to this work.
*Send correspondence to: luoyang@kmmu.edu.cn, dszou@cqu.edu.cn, yangjichun@cqu.edu.cn

**Table of Contents**

**Table S1** DNA oligonucleotides sequences used in this study

**Table S2** Mathematical formula for the cascade amplification of the FTO-switched nanoprobe

**Table S3** Comparison of various strategies for living cell imaging.

**Table S4** The detailed clinical information of clinical samples

**Figure S1** The lowest free energy structures of Probe A and Probe A/Probe B Complex

**Figure S2** The lowest free energy structures of Probe C

**Figure S3** XPS spectra of Mn 2p of $MnO_2$ nanosheets

**Figure S4** Probe B optimization experiment

**Figure S5** Optimization of the reaction time

**Figure S6** Optimization of the reaction temperature

**Figure S7** Time-dependent intracellular imaging by this proposed method

**Figure S8** Cell proliferation assay for the investigation of cytotoxicity of $MnO_2$ nanosheets

**Figure S9** Comparison of the flow cytometric mean fluorescence intensity data in MCF-7 and MCF-10A cells using the FTO-switched nanoprobe and the non-FTO-switched nanoprobe.

**Figure S10** The flow cytometric mean fluorescence intensity data in MCF-7, Hela and MCF-10A cells using the FTO-switched nanoprobe

**Figure S11** Application of the FTO-switched nanoprobe in the clinic

**Supporting tables**

**Table S1.** DNA oligonucleotides sequences used in this study

| Probe name | Sequence(5'-3') |
|---|---|
| non-FTO-switched probe A | TCATCTCTTCTCCGAGCCGGTCGAAATAGTAGCTTATC AGACTGATG |
| Probe A | TCATCTCTTCTCCG/6-MedA/GCCGGTCGAAATAGTAGCTTATCAGACTGATG |
| Probe C | FAM-TCAACATCAGTCATAAAGCTACTAT/rA/GGAAGAGATG ACTAGCTTATCAGACTGATGTTGA-BHQ1 |
| Cleavaged Probe C | GGAAGAGATGACTAGCTTATCAGACTGATGTTGA |
| Probe B-1 | TCAACATCAGTCTGATAAGCTACTATTT |
| Probe B-2 | TCAACATCAGTCTGATAAGCTACTATT |
| Probe B-3 | TCAACATCAGTCTGATAAGCTACTAT |
| Probe B-4 | TCAACATCAGTCTGATAAGCTACTA |
| Probe B-5 | TCAACATCAGTCTGATAAGCTACT |
| Probe B-6 | TCAACATCAGTCTGATAAGCTAC |
| Forward primer of miRNA-21 | GCCGCTAGCTTATCAGACTGATGT |
| Reverse primer of miRNA-21 | GTGCAGGGTCCGAGGT |
| Reverse transcription primer of miRNA-21 | GTCGTATCCAGTGCAGGGTCCGAGGTATTCGCACTGGA TACGACTCAACA |
| Forward primer of U6 | CTCGCTTCGGCAGCACA |
| Reverse primer of U6 | AACGCTTCACGAATTTGCGT |
| miRNA-21 | UAGCUUAUCAGACUGAUGUUGA |
| miRNA-155 | UUAAUGCUAAUCGUGAUAGGGGU |
| Let-7a | UGAGGUAGUAGGUUGUAUAGUU |
| miRNA-122 | UGGAGUGUGACAAUGGUGUUUG |
| miRNA-31 | AGGCAAGAUGCUGGCAUAGCU |
| miRNA-27a | UUCACAGUGGCUAAGUUCCGC |
| SS-FAM | FAM-ATACGG GCTGAG GCGATG GCATTT |

**Table S2.** The mathematical formula for the cascade amplification of the FTO-switched nanoprobe.

In the presence of sufficient FTO enzymes in the cell, if only X microRNA is added to the nanosystem, then theoretically X active DNAzyme can be generated through displacement reaction, and X active DNAzyme is believed to be able to cut px hairpin substrates. Meanwhile, $Mn^{2+}$ can be considered to have a q-fold enhancement effect compared with $Mg^{2+}$. The theoretical amplification efficiency is calculated as follows:

| Recycle No. | Number of Target | Outcome signal | Total number of output Fluorescence signals |
|---|---|---|---|
| 0 | x | 0 | 0 |
| 1 | x | pqx | pqx |
| 2 | x(pq+1) | pqx(pq+1) | pqx+pqx(pq+1) |
| … | … | … | … |
| n | $x(pq+1)^{n-1}$ | $pqx(pq+1)^{n-1}$ | $x(pq+1)[(pq+1)^{n-1}-1]$ |

Finally, when the recycle No. is n, the total number of output fluorescence signals is x(pq+1)[(pq+1)n-1-1], which indicates that the DNA circuit is in an exponential amplification mode.

**Table S3.** Comparison of various strategies for living cell imaging.

| Strategies | Signal amplification method | Controllability | LOD | Refs |
|---|---|---|---|---|
| The proposed method | DNAzyme | GSH-FTO | 9.7 pM | - |
| NIR controllable DNA walker | DNA walker | NIR | 100 pM | 1 |
| Smart Hairpins@$MnO_2$ Nanosystem | Enzyme-free exponential amplification | GSH | 33 fM | 2 |
| DNAzyme HIFU probe | DNAzyme | HIFU | 345 nM | 3 |
| Self-protected DNAzyme walker | Promoted DNAzyme | None | 10 pM | 4 |
| DNAzyme-recycling amplification | DNAzyme | GSH | 100pM | 5 |
| DNA Cross-Linked Polymeric | Hybridization chain reaction | None | 4.4 pM | 6 |
| Self-Powered FRET Flares | Catalytic hairpin assembly | AS1411 | 25 pM | 7 |
| Autonomous DNA Nanomachine | DNA walker | pH and NIR | 19.4 pM | 8 |

**Table S4.** The detail clinical information of clinical samples, including breast cancer patients (BC) patients and healthy donors (HD) .

| Sample | Age | Gender | Tumor staging | HER2 status (immunohistochemistry) |
|---|---|---|---|---|
| HD1 | 28 | Female | - | - |
| HD2 | 34 | Female | - | - |
| HD3 | 57 | Female | - | - |
| HD4 | 38 | Female | - | - |
| HD5 | 60 | Female | - | - |
| BC1 | 55 | Female | II | +++ |
| BC2 | 45 | Female | III | +++ |
| BC3 | 67 | Female | I | ++ |
| BC4 | 39 | Female | II | ++ |
| BC5 | 68 | Female | IV | +++ |

## Supporting Figures

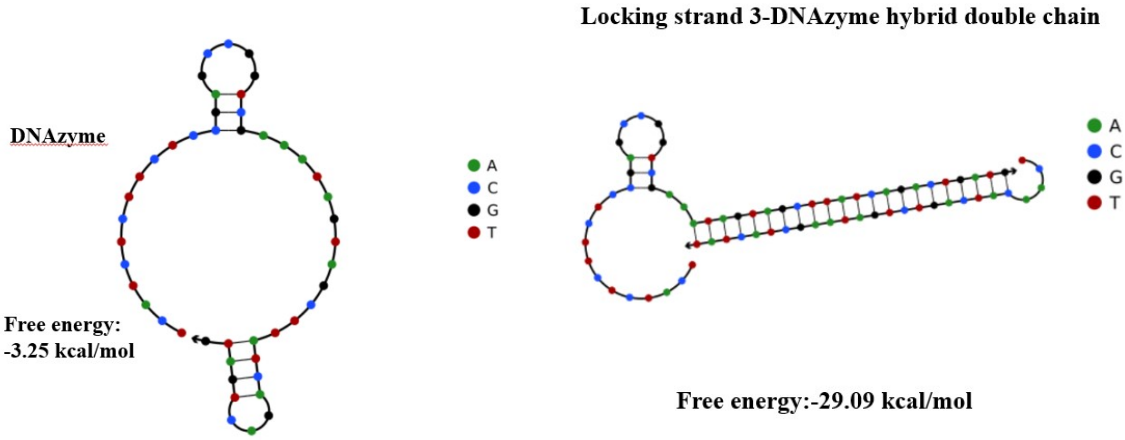


**Figure S1.** The lowest free energy structures of Probe A(left) and Probe A/Probe B Complex(right). As shown in the secondary structure, Probe B(Probe B-3) can be well integrated with the recognition region on one side of Probe A, and the target recognition site is retained at the convex end. They are predicted by NUPACK (www.nupack.org) at 37 $^{o}$C .

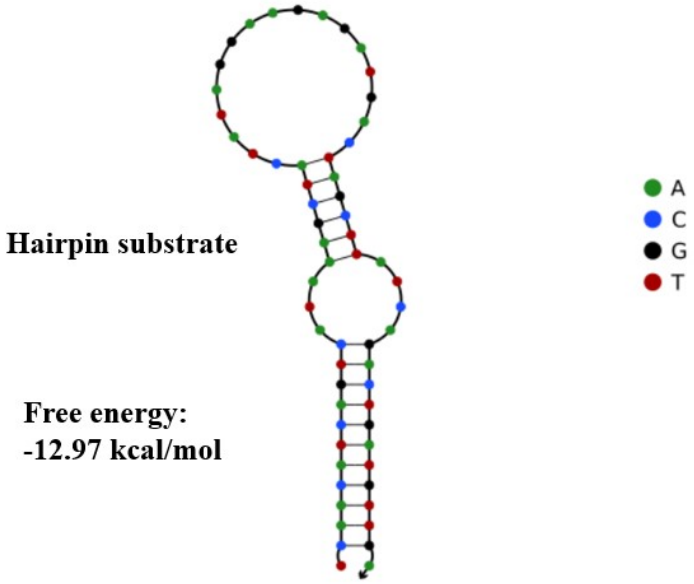


**Figure S2.** The lowest free energy structures of Probe C. It is predicted by NUPACK (www.nupack.org) at 37 ºC.

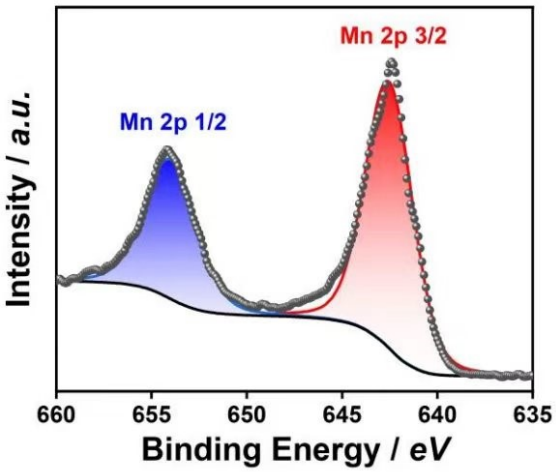


**Figure S3.** XPS spectra of Mn 2p of $MnO_2$ nanosheets.

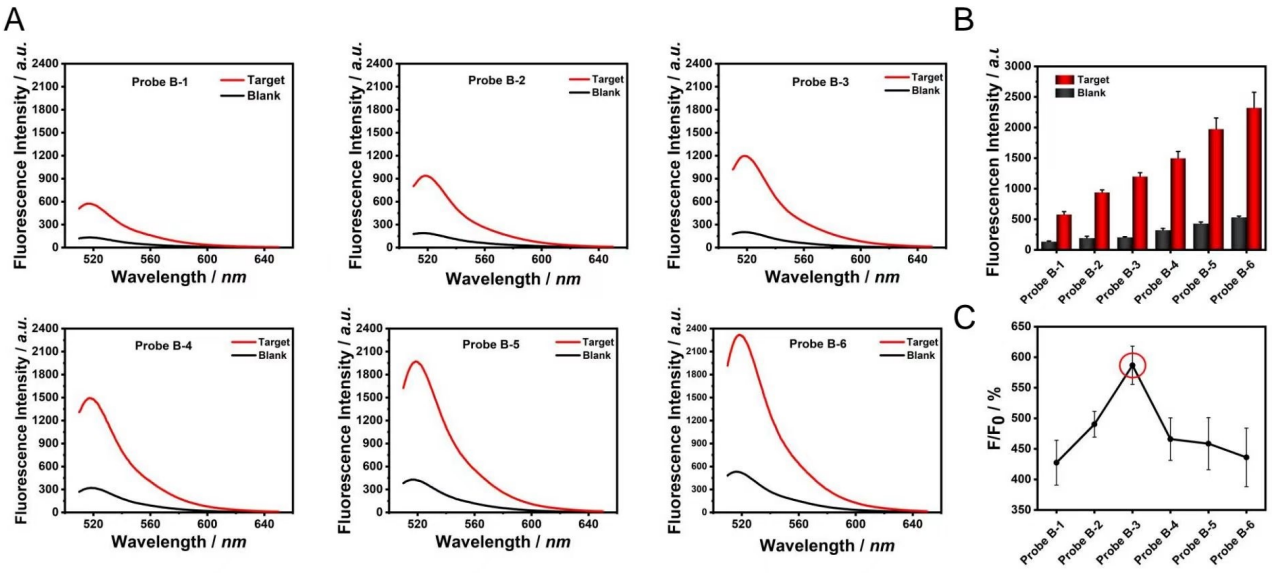


**Figure S4.** Probe B optimization experiment. (A) Fluorescence spectra of Probe A with Probe B of different lengths (Probe B-1 to Probe B-6) in the presence (red line) or absence (black line) of the 150 nM target initiator. (B) Peak fluorescence intensity and (C) signal-to-noise ratio of different Probe A in the presence (F) and absence (F0) of target initiator. Probe B-3 is used in subsequent experiments unless otherwise stated. Error bars represent mean ±SD (n = 3).

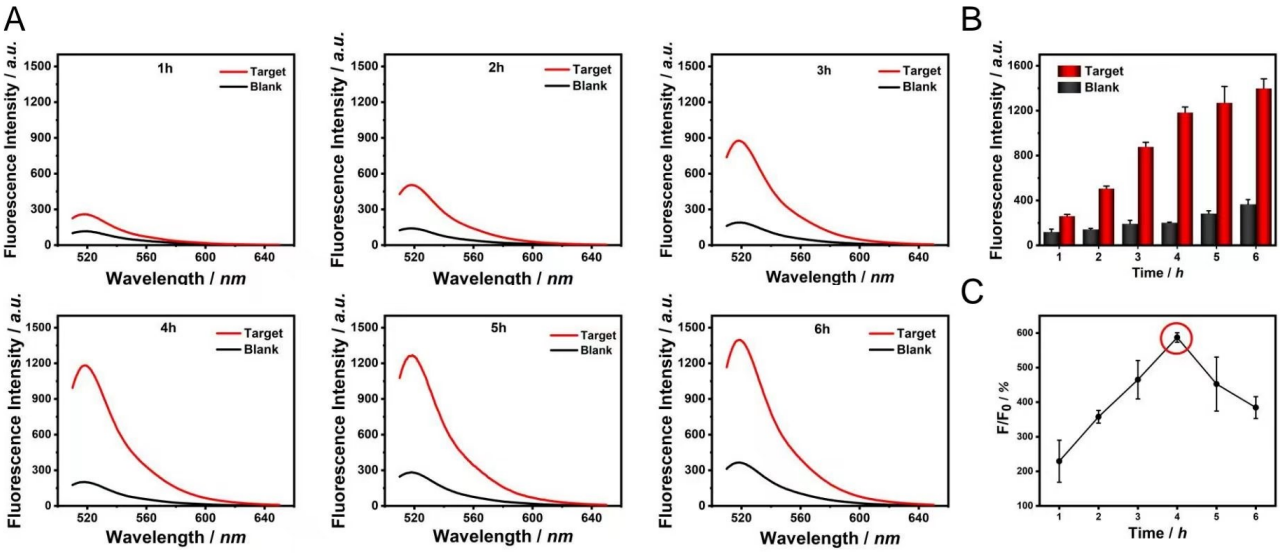


**Figure S5.** Optimization of the reaction time. (A) The fluorescence spectra of Probe A in the presence (red line) and absence (black line) of the target microRNA after 1 to 6 h incubation. (B) Peak fluorescence intensity and (C) signal-to-noise ratio of the samples in pane A. 4 h is used in subsequent experiments unless otherwise stated. Error bars represent mean ±SD (n = 3).

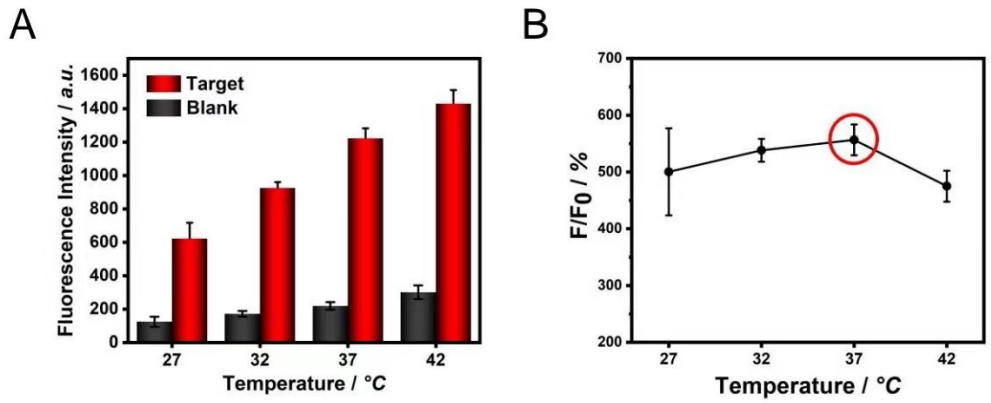


**Figure S6.** Optimization of the reaction temperature. 37°C is used in subsequent experiments unless otherwise stated. Error bars represent mean ±SD (n = 3).

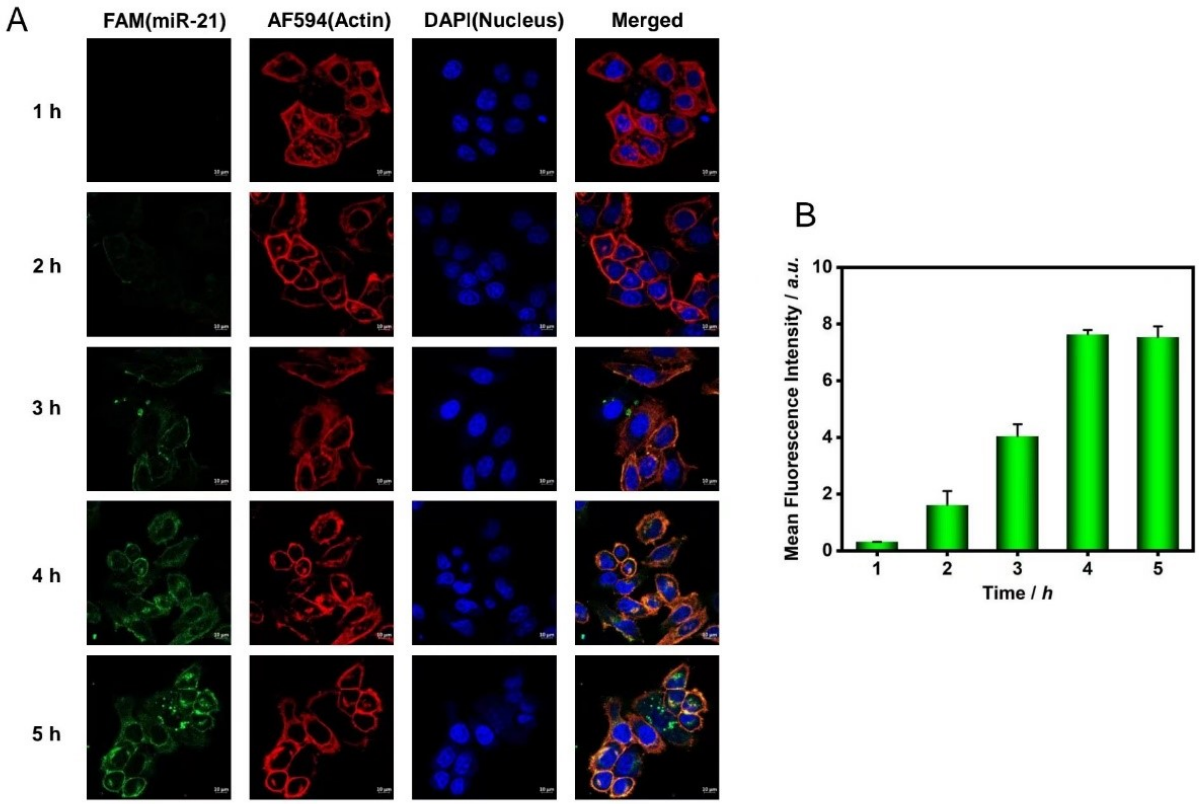


**Figure S7.** Time-dependent intracellular imaging by this proposed method. (A) Confocal fluorescence images of MCF-7 cells and (B) the mean fluorescence intensity of the corresponding cells detected by the FTO-switched nanoprobe with different incubation time. Error bars represent mean ±SD (n = 3).

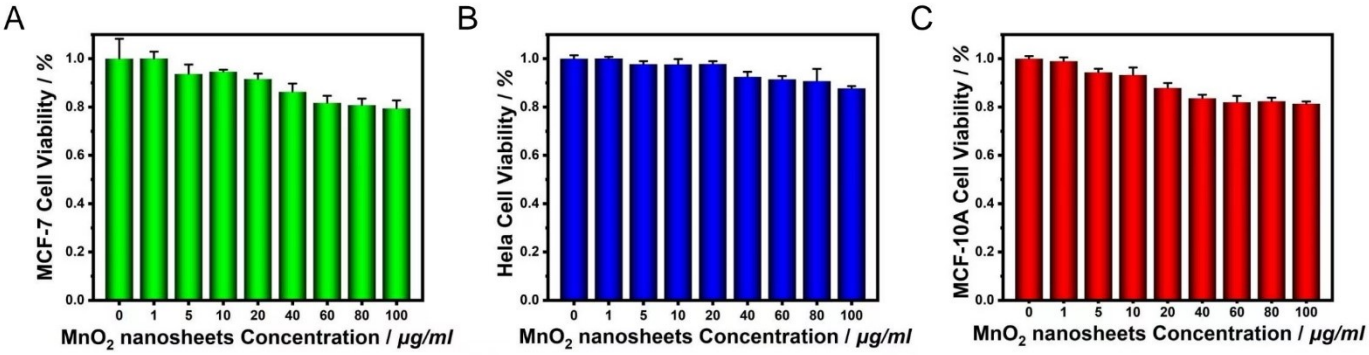


**Figure S8.** Cell proliferation assay for the investigation of cytotoxicity of $MnO_2$ nanosheets. The cell viability values (%) are determined by incubating (A) MCF-7 cells, (B) Hela cells and (C) MCF-10A cells with $MnO_2$ nanosheets of varied concentrations (0-100 μg/mL) for 24 h. Error bars represent means ± SD (n = 3).

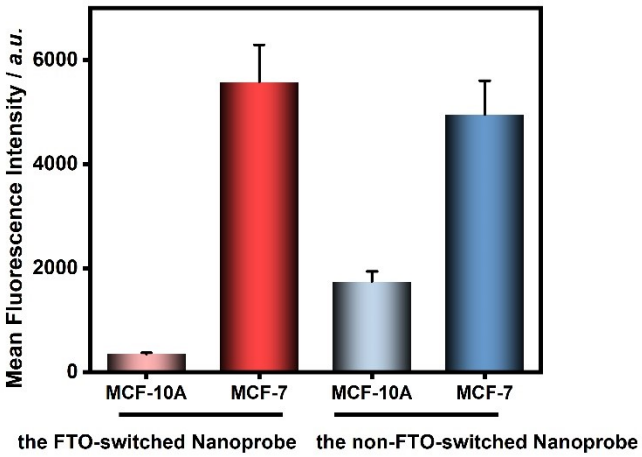


**Figure S9.** Comparison of the flow cytometric mean fluorescence intensity data in MCF-7 and MCF-10A cells using the FTO-switched nanoprobe and the non-FTO-switched nanoprobe. The data error bars indicate mean ± SD (n=3).

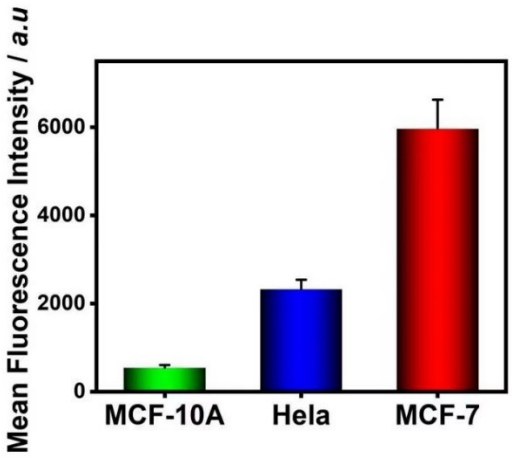


**Figure S10.** The flow cytometric mean fluorescence intensity data in MCF-7, Hela and MCF-10A cells using the FTO-switched nanoprobe. The data error bars indicate mean ± SD (n=3).

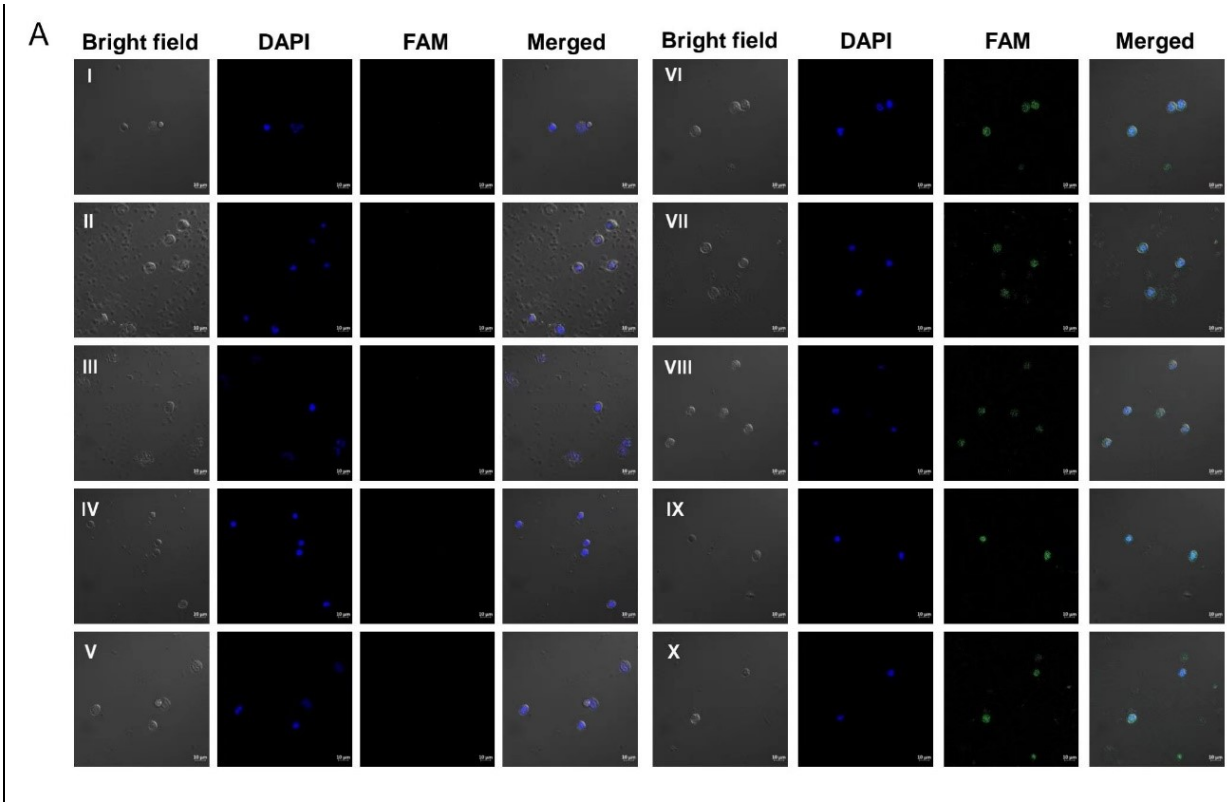

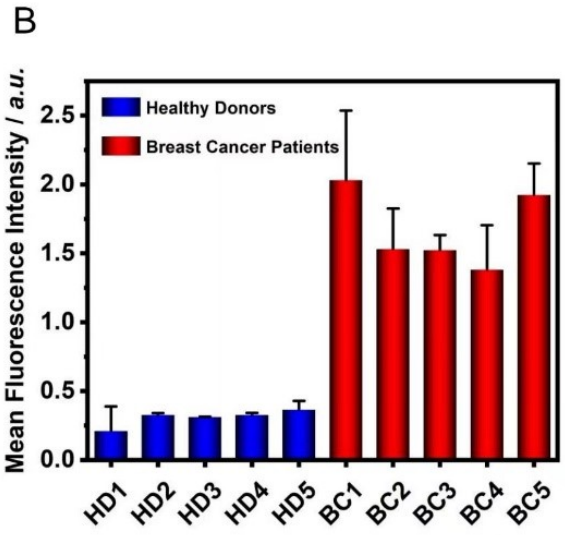


**Figure S11.** Application of the FTO-switched nanoprobe in the clinic. (A) Confocal fluorescence imaging of the samples from healthy individuals (I-V) and breast cancer patients (VI-X). The scale bar is 10 μm. (B) The results of circulating tumor cells were detected by the FTO-switched nanoprobe in 10 samples.

**REFERENCE**

**1**. M. Ye, Y. Kong, C. Zhang, Y. Lv, S. Cheng, D. Hou and Y. Xian, *ACS Nano*, 2021, **15**, 14253-14262.
**2**. Z. Z. Yang, B. R. Liu, T. Huang, B. P. Xie, W. J. Duan, M. M. Li, J. X. Chen, J. Chen and Z. Dai, *Analytical Chemistry*, 2022, **94**, 8014-8023.
**3**. X. Wang, G. Kim, J. L. Chu, T. Song, Z. Yang, W. Guo, X. Shao, M. L. Oelze, K. C. Li and Y. Lu, *J Am Chem Soc*, 2022, **144**, 5812-5819.
**4**. Y. Gao, S. Zhang, C. Wu, Q. Li, Z. Shen, Y. Lu and Z. S. Wu, *ACS Nano*, 2021, **15**, 19211-19224.
**5**. R. Wang, S. Wang, X. Xu, W. Jiang and N. Zhang, *Anal Chim Acta*, 2021, **1149**, 338213.
**6**. F. Yang, S. Li, X. Li, R. Yuan and Y. Xiang, *Analytical Chemistry*, 2022, **94**, 8014-8023.
**7**. J. Li, A. Wang, X. Yang, K. Wang and J. Huang, *Anal Chem*, 2021, **93**, 6270-6277.
**8**. J. L. Gao, Y. H. Liu, B. Zheng, J. X. Liu, W. K. Fang, D. Liu, X. M. Sun, H. W. Tang and C. Y. Li, *ACS Appl Mater Interfaces*, 2021, **13**, 31485-31494.